ELSEVIER

Computers and Geotechnics 29 (2002) 451–475

COMPUTERS AND GEOTECHNICS

www.elsevier.com/locate/compgeo

A practical method for solving free-surface seepage problems

Jean-Pierre Bardet*, Tetsuo Tobita

Civil Engineering Department, University of Southern California, Los Angeles, CA 90089-2531, USA

Received 1 October 2001; received in revised form 21 January 2002; accepted 6 February 2002

Abstract

Free-surface (unconfined) seepage problems are commonly encountered in geotechnical engineering. In these problems, the determination of the free surface usually requires sophisticated numerical techniques, unfamiliar to most engineers and students. Herein we present a practical finite difference method for unconfined seepage, which can be easily implemented in spreadsheets. The finite difference equations are based on the concepts of extended pressure and flux conservation. The method is illustrated by several free-surface seepage problems previously analyzed with more sophisticated numerical techniques. The proposed method eliminates the formation of matrix systems at the expenses of slower convergence rate for large problems. It has not only educational but also practical values as it applies to various engineering problems.

Keywords: Seepage; Finite differences; Unconfined flow; Free surface; Permeability; Spreadsheets

1. Introduction

Free-surface seepage problems are commonly encountered in the practice of geotechnical engineering. In these problems, the free-surface that delimits the flow boundaries can be found using nonlinear numerical techniques including finite difference method with adaptive mesh [1], finite element method with adaptive mesh (e.g. [2–4]) and fixed mesh (e.g. [5–13]). Among all the proposed methods proposed for solving free-surface seepage problems, the "Extended Pressure" (EP) method initially proposed by Brezis et al. [14] emerges one of the most efficient as it reduces variational inequalities to simpler equalities through an extension of Darcy's law.

* Corresponding author.
E-mail address: bardet@usc.edu (J.-P. Bardet).

0266-352X/02/$ - see front matter
PII: S0266-352X(02)00003-4

The EP method was applied to various types of free-surface seepage problems and numerical solution schemes (e.g. [9,15,16]).

The numerical methods for solving free-surface seepage problems are however not commonly used in engineering practice and largely ignored in soil mechanics textbooks, mainly because they require rather complicated derivations and implementations. Some textbooks (e.g. [17]) present basic spreadsheet solutions for confined seepage problems with multiple soil layers and anisotropic permeability. However, these basic spreadsheet techniques are limited to confined seepage problems for which the flow boundaries are known. At the present, they do not apply to unconfined seepage problems, such as free-surface flows within earthdams.

Hereafter we propose a practical finite difference approach for calculating unconfined seepage using spreadsheets. We derive the finite difference equations using flux conservation in the general case of nonuniform and anisotropic permeability and boundary conditions. The method proposed hereafter has not only educational values as it describes openly the equations used in solving free-surface seepage problems, but also practical values as it is applicable to many free-surface seepage problems.

2. Theory

2.1. Review of seepage theory

The two-dimensional flow of water through porous soils is assumed to follow Darcy's relation [18]:

$$\begin{pmatrix} v_x \\ v_y \end{pmatrix} = -\begin{pmatrix} k_x & k_{xy} \\ k_{xy} & k_y \end{pmatrix} \begin{pmatrix} \dfrac{\partial h}{\partial x} \\ \dfrac{\partial h}{\partial y} \end{pmatrix} \quad \text{or} \quad \mathbf{v} = -\mathbf{K} \quad \mathbf{grad}(h) \tag{1}$$

where k_x, k_y and k_{xy} are coefficients of the permeability matrix $\mathbf{K}$, h is the total head, and v_x and v_y are the components of the discharge velocity vector $\mathbf{v}$. Hereafter we consider only the cases of isotropic permeability ($k_x = k_y$) and anisotropic permeability ($k_x \neq k_y$) that have the x- and y-axis for principal axes (i.e. $k_{xy} = 0$). In the case of steady flow of water, the conservation of water mass leads to the following partial differential equation:

$$\frac{\partial v_x}{\partial x} + \frac{\partial v_y}{\partial y} = 0 \quad \text{or} \quad \mathrm{div}(\mathbf{v}) = 0 \tag{2}$$

Eq. (2) can also be expressed as:

$$\int_S \mathbf{v}.\mathbf{n} \; dS = 0 \tag{3}$$

where S is a closed line and $\mathbf{n}$ is the unit vector normal to S. Eqs. (1) and (2) lead to the well-known partial differential equation:

$$k_x \frac{\partial^2 h}{\partial x^2} + k_y \frac{\partial^2 h}{\partial y^2} = 0 \tag{4}$$

which further reduces to Laplace equation in the case of isotropic permeability ($k_x = k_y$).

2.2. Finite difference equations for confined seepage

The finite difference equations for seepage can be formulated (1) from Eq. (4) using the second order derivatives of h (e.g. [17]), or (2) more efficiently from Eq. (3) using the first order derivative of h. As shown in Fig. 1, when S is taken as $A_2\ A_4\ A_6\ A_8$ for irregular and rectangular finite difference grids, Eq. (3) leads to the following finite difference equation:

$$\begin{aligned} &\frac{h_{i,j} - h_{i-1,j}}{\Delta x_1}(k_{x1}S_1 + k_{x8}S_8) - \frac{h_{i+1,j} - h_{i,j}}{\Delta x_2}(k_{x4}S_4 + k_{x5}S_5) + \\ &\frac{h_{i,j} - h_{i,j-1}}{\Delta y_1}(k_{y2}S_2 + k_{y3}S_3) - \frac{h_{i,j+1} - h_{i,j}}{\Delta y_2}(k_{y6}S_6 + k_{y7}S_7) = 0 \end{aligned} \tag{5}$$

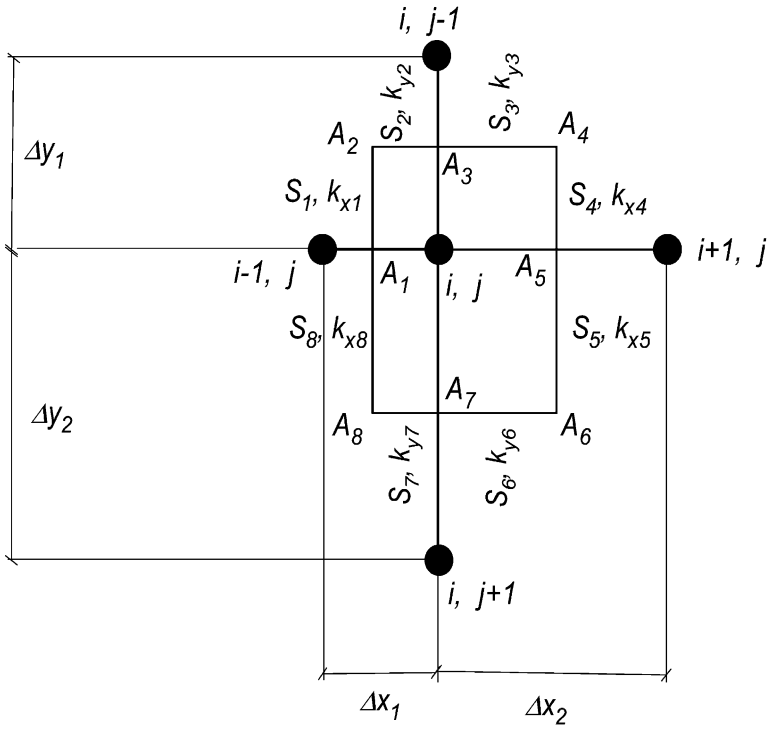

Fig. 1. Grid geometry used for derivation of finite difference equations using flux conservation.

where $h_{i,j}$, $h_{i-1,j}$, $h_{i+1,j}$, $h_{i,j-1}$, and $h_{i,j+1}$ are the values of total head h at grid nodes; S_1, S_2,..., S_8 are the segments A_1A_2, A_2A_3, ..., A_8A_1; Δx_1 and Δx_2 are the grid spacing in the x-direction; Δy_1 and Δy_2 are the grid spacing in the y-direction; k_{x1}, k_{x4}, k_{x5}, and k_{x8} are the permeability in the x-direction in the four quadrants surrounding the center node; and k_{y2}, k_{y3}, k_{y6}, and k_{y7} are the corresponding permeability in the y-direction. Eq. (5) can be rewritten as follows:

$$h_{i,j} = \frac{1}{D}\left(h_{i-1,j}\frac{k_{x1}S_1 + k_{x8}S_8}{\Delta x_1} + h_{i+1,j}\frac{k_{x4}S_4 + k_{x5}S_5}{\Delta x_2} + h_{i,j-1}\frac{k_{y2}S_2 + k_{y3}S_3}{\Delta y_1} + h_{i,j+1}\frac{k_{y6}S_6 + k_{y7}S_7}{\Delta y_2}\right) \tag{6}$$

where the coefficient D is:

$$D = \frac{k_{x1}S_1 + k_{x8}S_8}{\Delta x_1} + \frac{k_{x4}S_4 + k_{x5}S_5}{\Delta x_2} + \frac{k_{y2}S_2 + k_{y3}S_3}{\Delta y_1} + \frac{k_{y6}S_6 + k_{y7}S_7}{\Delta y_2} \tag{7}$$

Eq. (6) is second-order accurate when the element $A_2\ A_4\ A_6\ A_8$ is selected such as $S_2 = S_7 = \Delta x_1/2$; $S_3 = S_6 = \Delta x_2/2$; $S_1 = S_4 = \Delta y_1/2$; and $S_5 = S_8 = \Delta y_2/2$ because the first order derivatives of h are second-order accurate when evaluated at the middle of grid points. Through the selection of coefficients S_i, k_{xi}, k_{yi}, Δx_1, Δx_2, Δy_1, and Δy_2, Eq. (6) encompasses many cases of anisotropic permeability, layered permeability, and impervious boundary conditions. In the case of anisotropic permeability with different grid spacing in the x- and y-directions, i.e.:

$$\begin{aligned} &S_2 = S_3 = S_6 = S_8 = \Delta x/2;\ S_1 = S_8 = S_4 = S_5 = \Delta y/2; \\ &k_{x1} = k_{x3} = k_{x4} = k_{x5} = k_x; \quad k_{y2} = k_{y3} = k_{y6} = k_{y7} = k_y; \quad \text{and} \\ &\Delta x_1 = \Delta x_2 = \Delta x; \quad \Delta y_1 = \Delta y_1 = \Delta y \end{aligned} \tag{8}$$

Eq. (6) becomes:

$$h_{i,j} = \frac{1}{2(1+\beta)}\left(h_{i+1,j} + h_{i-1,j} + \beta\left(h_{i,j+1} + h_{i,j-1}\right)\right) \tag{9}$$

where the coefficient β is:

$$\beta = \frac{k_y}{k_x}\left(\frac{\Delta x}{\Delta y}\right)^2 \tag{10}$$

In the particular case of isotropic permeability and even grid spacing ($\beta = 1$), Eq. (9) reduces to the well-known finite difference equation:

$$h_{i,j} = \frac{1}{4}\left(h_{i+1,j} + h_{i-1,j} + h_{i,j+1} + h_{i,j-1}\right) \tag{11}$$

Eq. (6) applies to most cases of interfaces and boundary conditions after an appropriate selection of segments S_1 to S_8 and permeability coefficients k_{x1}, k_{x3}, etc...For instance, in the case of a vertical interface between two materials of isotropic permeability k_1 and k_2, i.e.:

$$\begin{aligned} &S_1 = \ldots = S_8 = \Delta x/2; \quad k_{x1} = k_{y2} = k_{x8} = k_{y7} = k_1; \\ &\Delta x_1 = \Delta x_2 = \Delta y_1 = \Delta y_1 = \Delta x \quad \text{and} \quad k_{x4} = k_{y3} = k_{x5} = k_{y6} = k_2 \end{aligned} \tag{12}$$

Eq. (6) becomes:

$$h_{i,j} = \frac{h_{i-1,j} + h_{i+1,j}\alpha + h_{i,j-1}(1+\alpha)/2 + h_{i,j+1}(1+\alpha)/2}{2(1+\alpha)} \quad \text{and} \quad \alpha = k_2/k_1 \tag{13}$$

Similar equations can be derived for horizontal and inclined interfaces, provided that those pass through grid points. Eq. (6) applies to impervious inclined and corner boundaries as well, again provided that those pass through grid points (e.g. [17]). In the case of an horizontal impervious boundary:

$$\begin{aligned} &S_5 = S_6 = S_7 = S_8 = 0; \quad k_{x1} = k_{x3} = k_{y2} = k_{y3} = k; \quad \text{and} \\ &\Delta x_1 = \Delta x_2 = \Delta y_1 = \Delta y_1 = \Delta x S_1 = S_2 = S_3 = S_4 = \Delta x/2 \end{aligned} \tag{14}$$

Eq. (6) becomes:

$$h_{i,j} = \frac{1}{4}\left(h_{i-1,j} + h_{i+1,j} + 2h_{i,j-1}\right) \tag{15}$$

It is also noted that (1) the sum of the coefficients of the finite difference equations [i.e. Eq. (6)] should always be equal to one, which is a basic requirement for preserving flux conservation, and that (2) Eq. (6) applies directly to impervious boundaries without the need for fictitious grid nodes.

2.3. Free-surface (unconfined) seepage

Free-surface seepage problems can be defined through the generic problem in Fig. 2. The saturated domain Ω_w is comprised between points $ABCDE$ whereas the dry domain Ω_d is located above the free surface AE, which has an unknown location. The governing equation and boundary conditions of the free-surface seepage problem of Fig. 2 are:

$$\text{div}(\mathbf{v}) = 0 \quad \text{and} \quad p \geqslant 0 \quad \text{in} \quad \Omega_w \tag{16}$$

$$\mathbf{v} = -\mathbf{K}.\mathbf{grad}(p + y) \tag{17}$$

$$p = 0 \quad \text{in} \quad \Omega_d \tag{18}$$

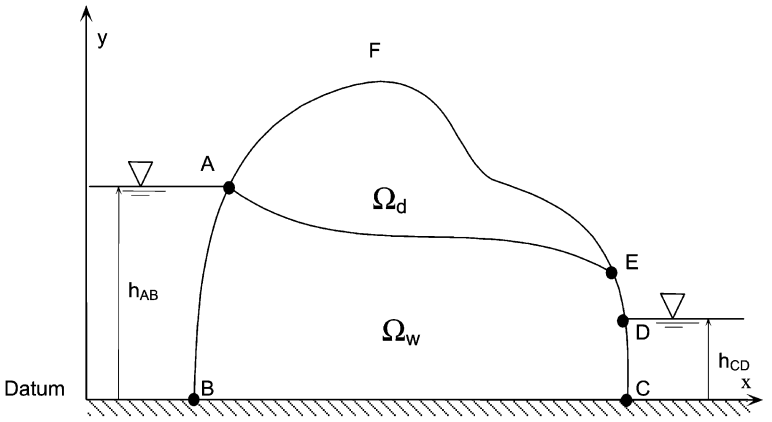

Fig. 2. A generic seepage problem with a free surface.

$$p = h_{AB} - y \text{ on AB and } p = h_{CD} - y \text{ on CD} \tag{19}$$

$$\mathbf{n}.\mathbf{v} = 0 \text{ on BC} \tag{20}$$

$$\mathbf{n}.\mathbf{v} = 0 \text{ and } p = 0 \text{ on AE} \tag{21}$$

$$\mathbf{n}.\mathbf{v} \leqslant \text{ and } p = 0 \text{ on DE} \tag{22}$$

where p is the pressure head; $\mathbf{n}$ represents the unit vector normal to the boundary; h_{AB} and h_{CD} are the water depth on the left and right side, respectively. In the solution of free-surface seepage problems, it is convenient to take the pressure head p as unknown instead of total head h. The pressure head p is related to water pressure u and water unit weight γ_w through $p = u/\gamma_w$. In their concept of "Extended Pressure" (EP), Brezis et al. [14] modifies Darcy's relation [i.e. Eq. (1)] as follows:

$$\mathbf{v}' = -\mathbf{K}[\mathbf{grad}(p) + H(p)\mathbf{grad}(y)] \tag{23}$$

where $\mathbf{v}'$ is the modified seepage velocity, and $H(p)$ is the Heaviside function:

$$H(p) = \begin{cases} 1 \text{ if } p \geqslant 0 \\ 0 \text{ if } p < 0 \end{cases} \tag{24}$$

When p is positive, Eq. (23) becomes identical to Eq. (17). In the EP framework, the new boundary value problem is made of Eqs. (19), (20) and (23) and the following equations:

$$p = 0 \text{ on DEFA} \tag{25}$$

$$\text{div}(\mathbf{v}') = 0 \text{ in } \Omega_w \cup \Omega_d \tag{26}$$

The mathematical derivations that establish the equivalence between the modified EP boundary value problem and the original free-surface seepage problem can be found in Brezis et al. [14] and Oden and Kikuchi [9]. For computational purposes, it is convenient to replace the Heaviside function H with the following ramp function H_ε:

$$H_\varepsilon(p) = \begin{cases} 1 \text{ if } p \geqslant \varepsilon \\ p/\varepsilon \text{ if } p < \varepsilon \end{cases} \tag{27}$$

When ε tends toward zero, H_ε tends towards H.

2.4. Finite difference equations for unconfined seepage

The finite difference equations for unconfined seepage, like those for confined seepage, can be conveniently derived using an area S surrounding a grid node:

$$-\int_S \mathbf{v}'.n\mathrm{d}\Gamma_c = \int_S \mathbf{K}.\mathbf{grad}(p)\mathrm{d}\Gamma_c + \int_S k_y H_\varepsilon(p) n_y \mathrm{d}\Gamma_c = 0 \tag{28}$$

For the grid shown in Fig. 1, the last integral of Eq. (28) is evaluated as follows:

$$\begin{aligned} \int_S k_y H_\varepsilon(p) n_y \mathrm{d}S &= (k_{y2}S_2 + k_{y3}S_3) H_\varepsilon\left[\frac{p_{i,j} + p_{i,j-1}}{2}\right] \\ &- (k_{y6}S_6 + k_{y7}S_7) H_\varepsilon\left[\frac{p_{i,j} + p_{i,j+1}}{2}\right] \end{aligned} \tag{29}$$

Therefore the finite difference equations for unconfined seepage is:

$$\begin{aligned} p_{i,j} = \frac{1}{D}\Bigg(& p_{i-1,j}\frac{k_{x1}S_1 + k_{x8}S_8}{\Delta x_1} + p_{i+1,j}\frac{k_{x4}S_4 + k_{x5}S_5}{\Delta x_2} + p_{i,j-1}\frac{k_{y2}S_2 + k_{y3}S_3}{\Delta y_1} \\ & + p_{i,j+1}\frac{k_{y6}S_6 + k_{y7}S_7}{\Delta y_2}\Bigg) + \frac{1}{D}\Bigg((k_{y2}S_2 + k_{y3}S_3) H_\varepsilon\left[\frac{p_{i,j} + p_{i,j-1}}{2}\right] \\ & - (k_{y6}S_6 + k_{y7}S_7) H_\varepsilon\left[\frac{p_{i,j} + p_{i,j+1}}{2}\right]\Bigg) \end{aligned} \tag{30}$$

In the case of evenly spaced square grid and anisotropic permeability, Eq. (30) becomes:

$$\begin{aligned} p_{i,j} = \frac{1}{2(1+\lambda)}\Big(& p_{i+1,j} + p_{i-1,j} + \lambda(p_{i,j+1} + p_{i,j-1}) \\ & + \lambda\Delta y\left[H_\varepsilon\left[\frac{p_{i,j} + p_{i,j-1}}{2}\right] - H_\varepsilon\left[\frac{p_{i,j} + p_{i,j+1}}{2}\right]\right]\Big) \end{aligned} \tag{31}$$

where $\lambda = k_x/k_y$. In the case of isotropic permeability ($\lambda = 1$), Eq. (31) further reduces to:

$$p_{i,j} = \frac{1}{4}\Big(p_{i+1,j} + p_{i-1,j} + p_{i,j-1} + p_{i,j+1} + \Delta y\Big[H_\varepsilon\Big[\frac{p_{i,j} + p_{i,j-1}}{2}\Big] - H_\varepsilon\Big[\frac{p_{i,j} + p_{i,j+1}}{2}\Big]\Big]\Big) \tag{32}$$

Compared to Eq. (11) for confined seepage, Eq. (32) for unconfined seepage has nonlinear H_ε terms, which render it slightly more complicated. Eq. (32) becomes linear and coincides with Eq. (11) when the values $(p_{i,j-1} + p_{i,j})/2$ and $(p_{i,j} + p_{i,j+1})/2$ are larger than ε. This corresponds to three grid nodes that are beneath the "smooth" free-surface, which is a concept specific to the EP method as illustrated later in an example.

2.5. Spreadsheet iterative calculations

In iterative spreadsheet calculations, the finite difference equations at all grid nodes are not written in a matrix format, which is the usual mathematical way to describe a system of n linear equations with n unknowns. Instead, the equations are written in cells (i.e. nodes) that relate the contents of adjacent cells. The equations are easily copied to other nodes (i.e. cells) by using the copying and pasting features of spreadsheets, which automatically increment row and column numbers. It is recommended to deactivate the iterative calculation feature of spreadsheets while defining the equations to avoid the temporary warning messages related to circular references, and to reactivate this iterative feature when all the equations are defined.

2.6. SOR solution

The iterative spreadsheet calculations are based on the numerical concept of successive relaxation (SR), which applies to the solution of both linear and nonlinear system of equations (e.g. [19,20]). The convergence of SR algorithm can be accelerated by using Successive Over-Relaxation (SOR). For instance, the SOR version of Eq. (11) is:

$$h_{i,j}^{m+1} = (1-\omega)h_{i,j}^{m} + \frac{\omega}{4}\left(h_{i+1,j}^{m} + h_{i-1,j}^{m} + h_{i,j+1}^{m} + h_{i,j-1}^{m}\right) \tag{33}$$

where ω is the relaxation factor, the value of which is usually taken between 1 and 2 for faster convergence. $h_{i,j}^{m}$ represents the value of $h_{i,j}$ at the mth iteration. Similarly the SOR version of Eq. (32) is:

$$p_{i,j}^{m+1} = (1-\omega)p_{i,j}^{m} + \frac{\omega}{4}\left(p_{i+1,j}^{m} + p_{i-1,j}^{m} + p_{i,j-1}^{m} + p_{i,j+1}^{m} + \Delta y\left[H_\varepsilon\left[\frac{p_{i,j}^{m} + p_{i,j-1}^{m}}{2}\right] - H_\varepsilon\left[\frac{p_{i,j}^{m} + p_{i,j+1}^{m}}{2}\right]\right]\right) \tag{34}$$

where $p_{i,j}^{m}$ represents the value of $p_{i,j}$ at the mth iteration. The mathematical analysis of stability and convergence of the SOR algorithm for free-surface seepage are

beyond the scope of this paper. As remarked in Oden and Kikuchi [9], it was found that the method converges when the parameter ε is selected not smaller than the grid spacing Δy.

Eq. (34) becomes in the case of (a) impervious bottom boundary:

$$p_{i,j}^{m+1} = (1-\omega)p_{i,j}^{m} + \omega\left(\frac{1}{4}(p_{i+1,j}^{m} + p_{i-1,j}^{m} + 2p_{i,j-1}^{m}) + \frac{\Delta y}{2}\right). \tag{35}$$

(b) left-hand-side impervious boundary:

$$\begin{aligned} p_{i,j}^{m+1} = {} & (1-\omega)p_{i,j}^{m} + \frac{\omega}{4}\left(2p_{i+1,j}^{m} + p_{i,j-1}^{m} + p_{i,j+1}^{m}\right. \\ & \left. + \Delta y\left[H_{\varepsilon}\left[\frac{p_{i,j}^{m} + p_{i,j-1}^{m}}{2}\right] - H_{\varepsilon}\left[\frac{p_{i,j}^{m} + p_{i,j+1}^{m}}{2}\right]\right]\right). \end{aligned} \tag{36}$$

(c) transition zone of horizontally varying permeability (k_1 to k_2, $a = k_2/k_1$):

$$\begin{aligned} p_{i,j}^{m+1} = {} & (1-\omega)p_{i,j}^{m} + \frac{\omega}{4}\left(\frac{2p_{i-1,j}^{m} + (1+\alpha)(p_{i,j-1}^{m} + p_{i,j+1}^{m}) + 2\alpha p_{i+1,j}^{m}}{1+\alpha}\right. \\ & \left. + \Delta y\left[H_{\varepsilon}\left[\frac{p_{i,j}^{m} + p_{i,j-1}^{m}}{2}\right] - H_{\varepsilon}\left[\frac{p_{i,j}^{m} + p_{i,j+1}^{m}}{2}\right]\right]\right) \end{aligned} \tag{37}$$

and (d) impervious bottom boundary in the transition zone of horizontally varying permeability (k_1 to k_2, $a = k_2/k_1$):

$$p_{i,j}^{m+1} = (1-\omega)p_{i,j}^{m} + \frac{\omega}{2}\left(\frac{p_{i-1,j}^{m} + (1+\alpha)p_{i,j-1}^{m} + \alpha p_{i+1,j}^{m}}{1+\alpha} + \Delta y H_{\varepsilon}\left[\frac{p_{i,j}^{m} + p_{i,j-1}^{m}}{2}\right]\right). \tag{38}$$

2.7. Flow lines and flow nets

For both confined and unconfined isotropic and anisotropic seepage problems, the flow lines can be obtained using the flow function ψ, which is directly obtainable from the values of total head at grid point. By definition, the flow function ψ is:

$$v_x = \frac{\partial \psi}{\partial y} \text{ and } v_y = -\frac{\partial \psi}{\partial x}$$

The quantity of seepage $\mathrm{d}q$ through a small element with side $\mathrm{d}x$ and $\mathrm{d}y$ is:

$$\mathrm{d}q = v_x \mathrm{d}y - v_y \mathrm{d}x = \mathrm{d}\psi \tag{39}$$

Therefore the quantity of seepage Δq between two adjacent nodes (i, j) and $(i, j+1)$ is:

$$\Delta q = \int_{i,j+1}^{i,j} v_x \mathrm{d}y = \frac{k_x}{4}\left(h_{i+1,j} - h_{i-1,j} + h_{i+1,j+1} - h_{i-1,j+1}\right) = \Delta\psi = \psi_{i,j} - \psi_{i,j+1} \tag{40}$$

The values of $\psi_{i,j}$ are usually set equal to zero along one of the boundary flow lines. After the calculation of $h_{i,j}$ the values of $\psi_{i,j}$ are calculated for each cell moving away from the boundary flow lines where$\psi_{i,j}=0$. Flow nets, which are superimpositions of flow lines and equipotential lines, can therefore be drawn by contouring the values of flow function ψ_{ij} and total head h_{ij} using constant interval values.

3. Applications

The main features of the EP method are first illustrated in a one-dimensional problem, then the applicabilty of the proposed numerical method is examined in the cases of two-dimensional problems found in Oden and Kikuchi [9], Lacy and Prevost [15], and Borja and Kishnani [16].

3.1. One-dimensional water column with free surface

As shown in Fig. 3a, the principle of the EP method is illustrated by finding the distribution of pressure head p in the water column of height h when the pressure p is prescribed at the top and bottom of the water column, i.e.:

$$p = 0 \text{ at } y = 0 \text{ and } p = p^* \text{ at } y = h \tag{41}$$

Assuming that the y-coordinate is oriented downward and that $h>p^*$, the obvious solution of the physical problem is:

$$\begin{cases} p = 0 & y \leqslant h - p^* \\ p = p^* + y - h & y > h - p^* \end{cases} \tag{42}$$

where $h-p^*$ is the physical position of the free surface. In one-dimension, the EP method [i.e. Eq. (26)] formulates the problem of Fig. 3a as follows:

$$\begin{cases} \dfrac{\mathrm{d}^2 p}{\mathrm{d}y^2} - \dfrac{1}{\varepsilon}\dfrac{\mathrm{d}p}{\mathrm{d}y} = 0 & p \leqslant \varepsilon \\ \dfrac{\mathrm{d}^2 p}{\mathrm{d}y^2} = 0 & p > \varepsilon \end{cases} \tag{43}$$

The analytical solution of Eqs. (41) and (43) is:

$$\begin{cases} p = \dfrac{p^* - \varepsilon}{h - d}\varepsilon e^{-\frac{\mathrm{d}}{\varepsilon}}\left(\mathrm{e}^{\frac{y}{\varepsilon}} - 1\right) & p \leqslant \varepsilon \\ p = p^* + \dfrac{p^* - \varepsilon}{h - d}(y - h) & p > \varepsilon \end{cases}, \tag{44}$$

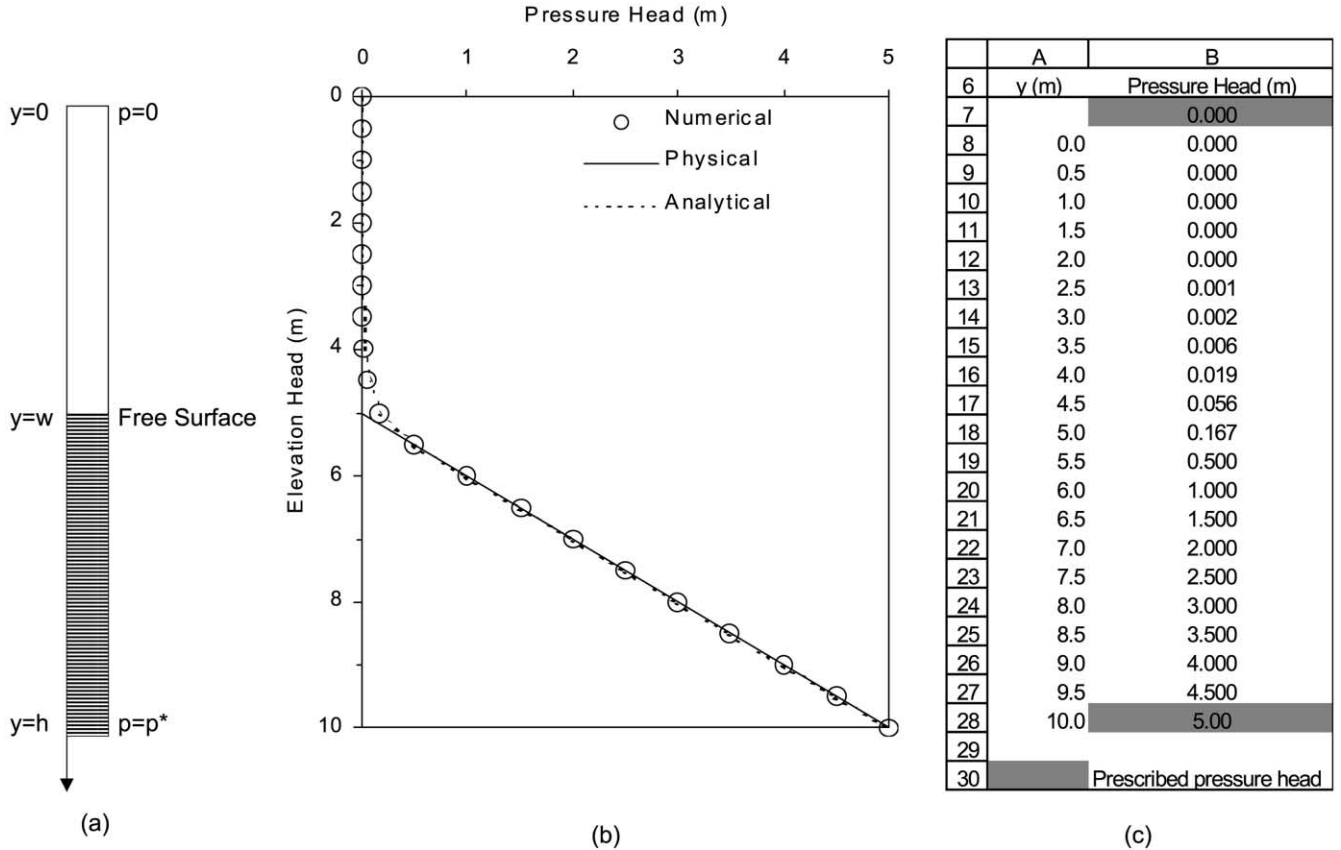

Fig. 3. One-dimensional water column with an unknown free surface: (a) geometry and boundary conditions; (b) comparison of numerical, physical and analytical solutions; and (c) spreadsheet used in numerical solution.

where d is the unknown y-value at which $p=\varepsilon$. The value d is determined from the continuity of p at $y=d$, i.e. by solving the following equation:

$$\frac{d}{\varepsilon}-\frac{h}{\varepsilon}=(1-\frac{p^*}{\varepsilon})(1-\mathrm{e}^{-\frac{d}{\varepsilon}}) \tag{45}$$

Eq. (43) excludes negative pressure as it assumes that p is between 0 and p^* in the water column. Fig. 3b compares the analytical [Eq. (44)] and physical [Eq. (42)] in the particular case: $\varepsilon=0.5$ m, $h=10$ m, and $p^*=5$ m. In this case, the solution of Eq. (45) is $d=5.5$ m. The EP solution displays a smooth transition of pressure head gradient between wet and dry domain, instead of a discontinuous slope as in the physical solution. The EP method therefore does not define exactly the position of the free surface. However, an approximate position can be inferred for the free surface by comparing analytical and physical solutions, i.e. by finding the pressure head p_w at depth $h-p^*$:

$$p_w=\varepsilon\frac{1-e^{\frac{h-p^*}{\varepsilon}}}{1-\mathrm{e}^{\frac{d}{\varepsilon}}} \tag{46}$$

In the particular example of Fig. 3b, $p_w=0.1389$. As shown in Fig. 4, p_w tends exponentially to ε/e when $(h-p^*)/\varepsilon$ becomes large ($e=2.718282$). Therefore, provided that the free surface remain far from an external boundary with prescribed pressure (i.e. $h>p^*$), the location of the free surface in the EP method corresponds to $p_w=\epsilon/e$. This relation, which was derived in one-dimension, is useful to obtain a

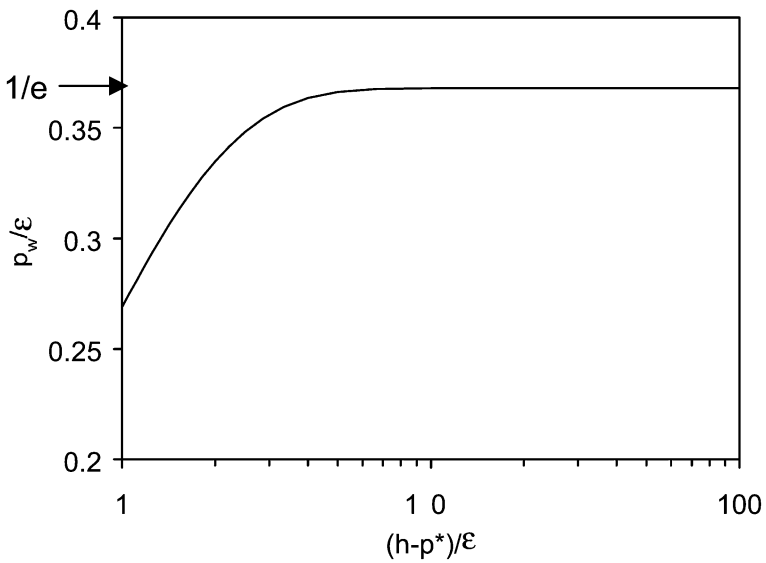

Fig. 4. Influence of the proximity between free surface and external boundary on the pressure p_w used for detection of free-surface position in EP method.

first-order approximation of the free-surface position for two-dimensional problems.

For one-dimensional free-surface seepage, the SOR version of finite difference equations are:

$$p_i^{m+1} = (1-\omega)p_i^m + \frac{\omega}{2}\left(p_{i+1}^m + p_{i-1}^m\right) + \frac{\omega}{2}\Delta y\left(H_\varepsilon\left[\frac{p_i^m + p_{i-1}^m}{2}\right] - H_\varepsilon\left[\frac{p_j^m + p_{i+1}^m}{2}\right]\right) \tag{47}$$

Fig. 3c shows the spreadsheet setup for the finite difference solution of Eqs. (41) and (43) using a grid spacing $\Delta y = 0.5$ m and an over-relaxation factor $\omega = 1.8$. The prescribed values of pressure head are in cells B7 and B28. As shown in Table 1, Eq. (47) becomes the spreadsheet formula of Table 1. It is entered first in cell B8 then copied to cell range B9:B27. The function H_ε, which is labeled H in Table 1, is implemented in Table 2 as a Visual Basic function [21]. As shown in Fig. 5, the

Table 1
Spreadsheet formulae used in examples

Eq. no.	Fig. no.	Cell	Spreadsheet formula
47	3, 4, 5	B8	=(1−w)*B8+w*(B7+B9)/2+w*DX/2*(H((B8+B7)/2,EPS)−H((B8+B9)/2,EPS))
34	6, 7	B6	=(1−W)*B6+w*(C6+B7+A6+B5)/4−+w*DX/4*(H((B7+B6)/2,EPS)− H((B6+B5)/2,EPS))
35		B25	=(1−w)*B25+w*((2*B24+C25+A25)/4+DX/2)
34	8	B7	=(1−w)*B7+w*(C7+B8+A7+B6)/4 +w*DX/4*(H((B6+B7)/2,EPS)− H((B7+B8)/2,EPS))
35		B29	=(1−w)*B29+w*((2*B28+C29+A29)/4+DX/2)
34	9	C7	=(1−w)*B7+w*(C7+B8+A7+B6)/4+w*DX/4*(H((B6+B7)/2,EPS)− H((B7+B8)/2,EPS))
35		B7	=(1−w)*B8+w*(2*C8+B9+B7)/4+w*DX/4*(H((B7+B8)/2,EPS)− H((B8+B9)/2,EPS))
36		B35	=(1−w)*B36+w*((2*B35+C36+A36)/4+DX/2)
34	10	B7	=(1−w)*B7+w*(C7+B8+A7+B6)/4+w*DX/4*(H((B6+B7)/2,EPS)− H((B7+B8)/2,EPS))
35		B28	=(1−w)*B28+w*((2*B27+C28+A28)/4+DX/2)
34	11	B7	=(1−w)*B7+w*(C7+B8+A7+B6)/4+w*DX/4*(H((B6+B7)/2,EPS)− H((B7+B8)/2,EPS))
35		B48	=(1−w)*B48+w*((2*B47+C48+A48)/4+DX/2)
37		L7	=(1−w)*L7+w*((2*K7+(1+a)*(L6+L8)+2*a*M7)/(4*(1+a))+ DX/4*(H((L6+L7)/2,EPS)−H((L7+L8)/2,EPS)))
38		L48	=(1−w)*L48+w*((K48+(1+a)*L47+a*M48)/(2*(1+a))+ DX/2*H((L47+L48)/2,EPS))

EPS = ε, DX = Δx, W = ω and a = α.

numerical solution converges toward the analytical solution [i.e. Eq. (44)], assuming that p is initially equal to zero at the beginning of iterations. After 25 iterations, the error between analytical and numerical solutions becomes smaller than 0.001.

3.2. Two-dimensional free-surface examples

3.2.1. Rectangular dam with tail water

Fig. 6a shows the geometry of the rectangular dam under investigation, and Fig. 7 displays the corresponding spreadsheet used in solving the free-surface problem. As shown in Fig. 7, the pressure head varies linearly on the left and right vertical boundaries, respectively. The prescribed pressure heads are entered in cell ranges A9:A29 and L25:L29. The pressure head is set equal to zero on the other boundary (i.e. cell ranges A6:A8, A6:K6 and L6:L25). A layer of grid points (i.e. A7:L7) was added onto the top of the original geometry in order to overcome the inaccurate

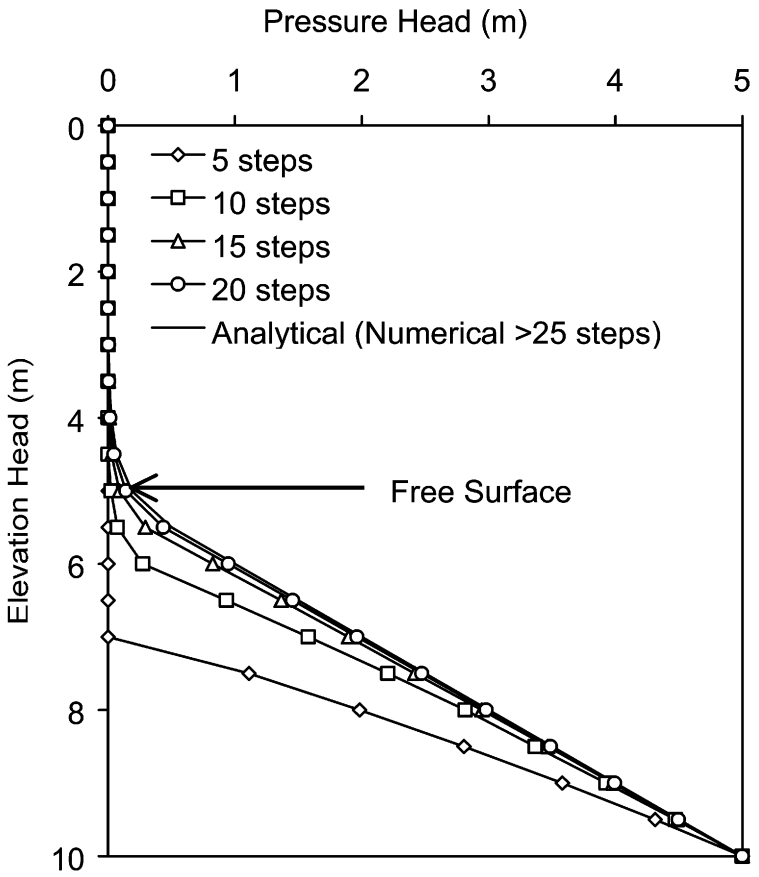

Fig. 5. Variation of computed pressure head p distribution with iteration number and analytical solution in the case of the one-dimensional water column example.

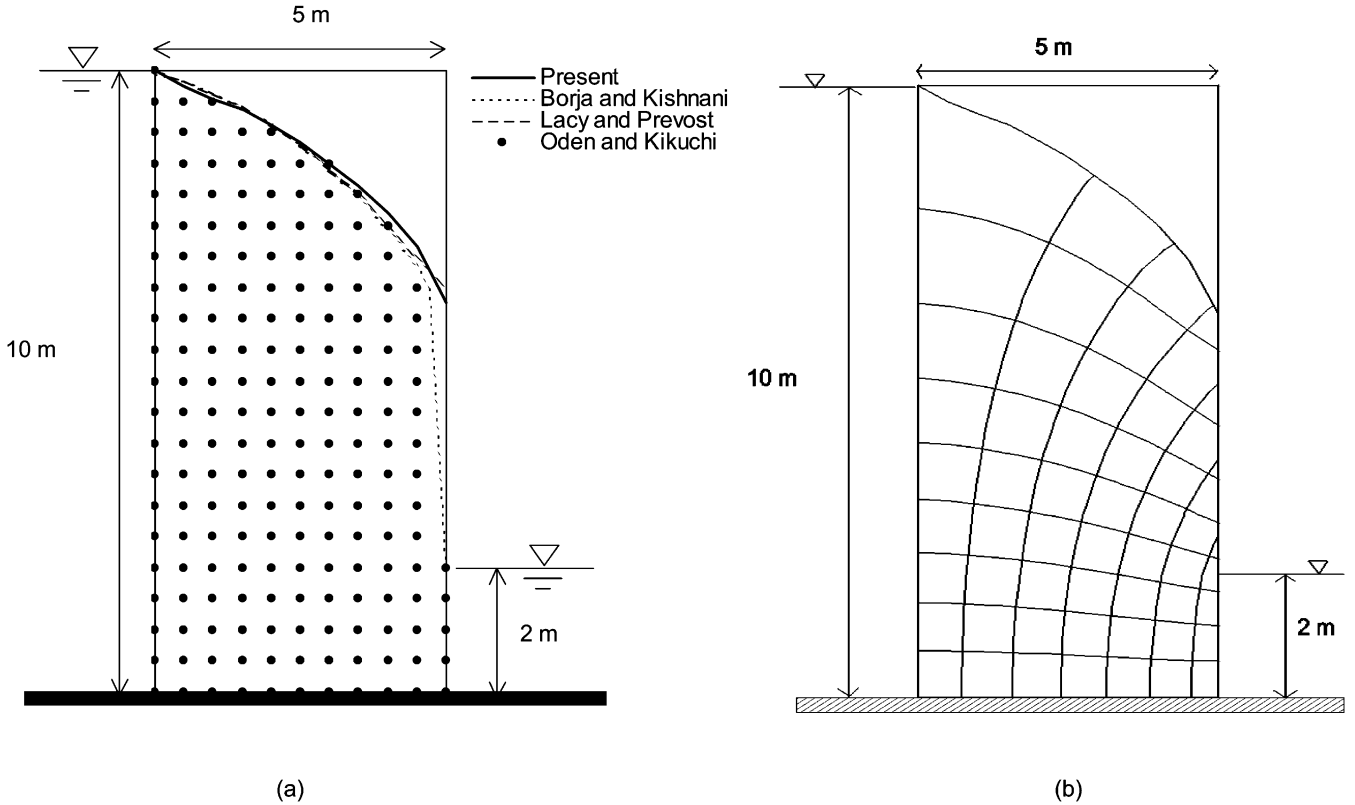

Fig. 6. (a) Rectangular dam with tail water: definition of problems and comparison of free surface obtained by present method; Oden and Kikuchi [9]; Lacy and Prevost [15]; and Borja and Kishnani [16]; (b) flow net.

	A	B	C	D	E	F	G	H	I	J	K	L
6	0	0	0	0	0	0	0	0	0	0	0	0
7	0	0.00	0.00	0.00	0.00	0.00	0.00	0.00	0.00	0.00	0.00	0
8	0	0.01	0.01	0.01	0.01	0.01	0.00	0.00	0.00	0.00	0.00	0
9	0	0.06	0.05	0.04	0.03	0.02	0.01	0.01	0.00	0.00	0.00	0
10	0.5	0.30	0.20	0.13	0.08	0.05	0.03	0.02	0.01	0.01	0.00	0
11	1	0.77	0.55	0.34	0.21	0.13	0.08	0.05	0.03	0.01	0.01	0
12	1.5	1.25	1.00	0.75	0.51	0.30	0.18	0.10	0.06	0.03	0.01	0
13	2	1.72	1.44	1.17	0.90	0.63	0.37	0.21	0.12	0.06	0.03	0
14	2.5	2.19	1.89	1.58	1.28	0.99	0.70	0.42	0.23	0.12	0.05	0
15	3	2.66	2.33	2.00	1.67	1.34	1.02	0.71	0.41	0.21	0.09	0
16	3.5	3.13	2.77	2.41	2.04	1.69	1.33	0.99	0.66	0.35	0.15	0
17	4	3.60	3.21	2.81	2.42	2.03	1.64	1.26	0.88	0.52	0.22	0
18	4.5	4.07	3.65	3.22	2.79	2.36	1.94	1.52	1.10	0.69	0.30	0
19	5	4.54	4.08	3.62	3.16	2.70	2.23	1.77	1.30	0.84	0.38	0
20	5.5	5.01	4.52	4.03	3.53	3.04	2.53	2.02	1.51	0.99	0.47	0
21	6	5.48	4.96	4.44	3.91	3.38	2.83	2.28	1.72	1.14	0.57	0
22	6.5	5.95	5.41	4.86	4.30	3.73	3.14	2.55	1.93	1.30	0.66	0
23	7	6.43	5.86	5.28	4.69	4.09	3.47	2.83	2.17	1.48	0.75	0
24	7.5	6.91	6.31	5.71	5.10	4.47	3.82	3.14	2.44	1.69	0.88	0
25	8	7.39	6.77	6.15	5.52	4.87	4.19	3.49	2.75	1.95	1.07	0
26	8.5	7.87	7.24	6.61	5.95	5.29	4.59	3.87	3.11	2.31	1.44	0.5
27	9	8.36	7.72	7.07	6.41	5.73	5.03	4.29	3.53	2.72	1.88	1
28	9.5	8.86	8.21	7.55	6.88	6.20	5.48	4.75	3.98	3.18	2.35	1.5
29	10	9.35	8.70	8.05	7.37	6.68	5.97	5.23	4.46	3.67	2.84	2
30												
31		Impervious boundary			Prescribed pressure head							

Fig. 7. Rectangular dam with tail water: spreadsheet representation and prescribed and converged values of pressure head.

determination of the free-surface as it gets too close to the top boundary at $x=0$, a drawback of the EP method which was pointed out in the one-dimensional water column example. The solution of the seepage problem of Fig. 6a requires only two types of finite difference equations, which are easily translated into the spreadsheet formulas of Table 1. Eq. (34) applies to cell range B7:K28, while Eq. (35) applies to cell range B29:K29. Eq. (34) is first entered in cells B7 then pasted into cell ranges B7:K28. Similarly Eq. (35) was entered in B29 and copied into range B29:K29. Table 3 lists the total number of equations, and the selected values of ε, Δx, and ω. The iterative calculations can be controlled by specifying a maximum number of iterations. They can also be stopped automatically by specifying a tolerance, i.e. when the change in p between two consecutive iterations becomes smaller than a given tolerance. As indicated in Table 3, the number of iterations required to converge was 135 for a tolerance set equal to 0.0001. The initial values of p were initially set equal to 0.0 and 0.3 at interior cells and bottom boundary cells, respectively. These initial values, which depend on the way the users copy and paste equations into cell ranges, slightly influence the number of iterations required to reach convergence. The values of converged pressure heads are shown in Fig. 7. As shown in Fig. 6a, the free surface corresponds to the value of pressure head equal to $p_w=\varepsilon/e$. The location of free surface computed by the proposed method agrees well with those found by Oden and Kikuchi [9], Lacy and Prevost [15], and Borja and Kishnani [16]. Table 4 lists model parameters and the number of iteration for the present

Table 2
Visual basic module for function H_ε

```
Function H(u As Single, eps As Single) As Single
 If u > eps Then
  H = 1#
 Else
  H = u / eps
 End If
End Function
```

Table 3
Values of parameters used in numerical examples: grid spacing Δx, EP parameter ε, SOR parameter ω, number of equations, number of iterations required to achieve convergence (tolerance is 0.0001 and $p_w=\varepsilon/e$ in all cases)

Fig. no.	Δx	ε	ω	Equations used	Total number of equations	Number of iterations
3, 4, 5	0.5	0.5	1.8	47	19	25
6, 7	0.5	0.5	1.2	34, 35	230	135
8	0.25	0.25	1.2	34, 35	540	275
9	0.25	0.25	1.2	34, 35, 36	580	500
10	0.25	0.25	1.2	34, 35	366	325
11	0.25	0.25	1.2	34, 35, 37, 38	882	414

Table 4
Comparison of model parameters and number of iteration for past and present methods applied to the example of Fig. 6

	$\Delta x = \Delta y$ (m)	ε (m)	Pressure head on free surface (m)	Relaxation factor ω	Number of iteration
Oden and Kikuchi [9]	0.5	0.1	0	1.7	20
Lacy and Prevost [15]	0.5	−0.13	−0.604	N.A.	11
Borja and Kishnani [16]	0.5	0.13	0.0 or 0.13	N.A.	4
Present method	0.5	0.5	0.184 ($=\varepsilon/e$)	1.2	135

method and Oden and Kikuchi [9], Lacy and Prevost [15], and Borja and Kishnani [16]. Oden and Kikuchi [9] reported their results by representing the finite element nodes inside and outside the flow domain. Lacy and Prevost [15], and Borja and Kishnani [16] traced the free surface by following some arbitrary pressure value (see Table 4). Fig. 6b shows the flow net obtained after calculating the flow function ψ at grid nodes [i.e. Eq. (40)], which is similar to that Lacy and Prevost [15] obtained using a more sophisticated method. As shown in Table 4, the SOR algorithm appears to converge more slowly than other methods when it is evaluated solely on the basis of number of iterations. However in contrast to the other methods, the SOR algorithm performs fewer operations as it does not require the reforming and inversion of a tangential matrix.

3.2.2. Rectangular dam with a toe drain

Fig. 8a shows the problem geometry of a rectangular dam with a toe drain, and Fig. 8b displays its spreadsheet representation and the prescribed and converged values of pressure heads. Some spreadsheet columns are hidden in Fig. 8b for the sake of conciseness. As in the previous example, Table 1 lists all the equations and spreadsheet formulas. Table 3 lists the values of parameters Δx, ε and ω. The total number of equations is 540. The number of iteration was 275, corresponding to initial values equal to 0.0 and 0.15 for interior cells and bottom boundary cells, respectively. As shown in Fig. 8a, there are small differences between the free surfaces found by the proposed method and those reported in Oden and Kikuchi [9], Lacy and Prevost [15] and Borja and Kishnani [16], especially as they become vertical at the to drain intersection, which is due to the limitations of the proposed method for locating the free surface and the coarse spatial discretization.

3.2.3. Rectangular dam with an impermeable sheet wall

Fig. 9a shows the problem geometry of a rectangular dam with an impermeable upstream wall sheet, and Fig. 9b displays its spreadsheet representation and the prescribed and converged values of pressure heads. Table 1 lists all formulae and Table 3 the values of parameters Δx, ε and ω. The total number of equation is 580. The number of iteration was 500, corresponding to initial values equal to 0.0 and 0.15 for interior cells and bottom boundary cells, respectively. As shown in Fig. 9a,

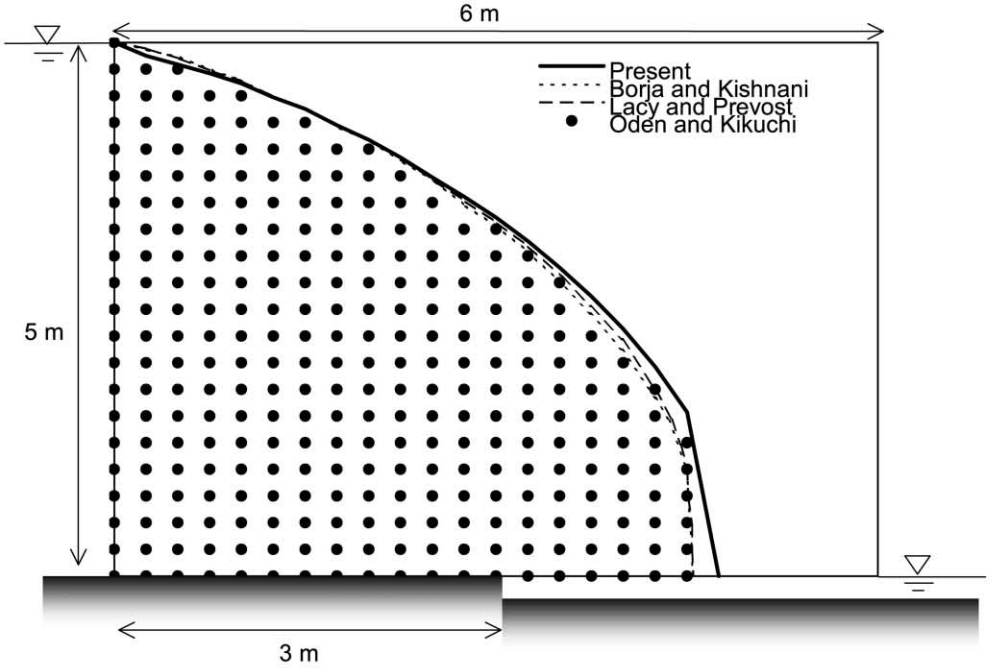

	A	B	M	N	Y	Z
6	0	0	0	0	0	0
7	0	0.00	0.00	0.00	0.00	0
8	0	0.01	0.00	0.00	0.00	0
9	0	0.03	0.00	0.00	0.00	0
10	0.25	0.16	0.00	0.00	0.00	0
11	0.5	0.40	0.00	0.00	0.00	0
12	0.75	0.64	0.01	0.00	0.00	0
13	1	0.88	0.01	0.01	0.00	0
14	1.25	1.12	0.03	0.02	0.00	0
15	1.5	1.36	0.06	0.04	0.00	0
16	1.75	1.61	0.12	0.07	0.00	0
17	2	1.85	0.21	0.12	0.00	0
18	2.25	2.09	0.35	0.21	0.00	0
19	2.5	2.33	0.48	0.33	0.00	0
20	2.75	2.57	0.60	0.45	0.00	0
21	3	2.81	0.71	0.55	0.00	0
22	3.25	3.05	0.82	0.64	0.00	0
23	3.5	3.29	0.91	0.72	0.00	0
24	3.75	3.53	0.99	0.77	0.00	0
25	4	3.78	1.04	0.81	0.01	0
26	4.25	4.02	1.08	0.80	0.01	0
27	4.5	4.27	1.09	0.73	0.01	0
28	4.75	4.51	1.07	0.54	0.01	0
29	5	4.76	1.09	0	0	0
30						
31		Impervious boundary				
32		Prescribed pressure head				

(b)

Fig. 8. (a) Rectangular dam with a toe drain: definition of problems and comparison of free surface obtained by present method; Oden and Kikuchi [9]; Lacy and Prevost [15]; and Borja and Kishnani [16]; (b) spreadsheet representation and prescribed and converged values of pressure head.

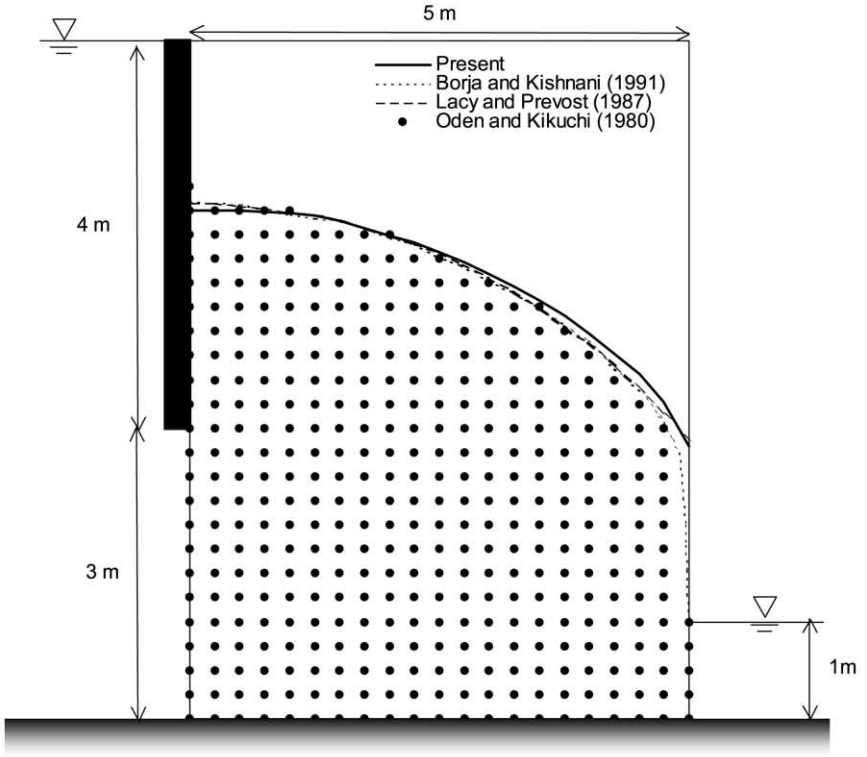

	A	B	C	U	V
6		0	0	0	0
7		0.00	0.00	0.00	0
8		0.00	0.00	0.00	0
9		0.00	0.00	0.00	0
10		0.00	0.00	0.00	0
11		0.00	0.00	0.00	0
12		0.01	0.01	0.00	0
13		0.03	0.03	0.00	0
14		0.09	0.09	0.00	0
15		0.29	0.28	0.00	0
16		0.56	0.55	0.00	0
17		0.84	0.83	0.00	0
18		1.15	1.13	0.00	0
19		1.47	1.46	0.01	0
20		1.83	1.81	0.01	0
21		2.24	2.20	0.02	0
22		2.73	2.64	0.04	0
23	4	3.42	3.12	0.07	0
24	4.25	3.84	3.51	0.10	0
25	4.5	4.16	3.85	0.14	0
26	4.75	4.45	4.16	0.18	0
27	5	4.72	4.44	0.22	0
28	5.25	4.98	4.71	0.28	0
29	5.5	5.23	4.97	0.33	0
30	5.75	5.49	5.23	0.39	0
31	6	5.74	5.48	0.49	0.00
32	6.25	5.99	5.74	0.67	0.25
33	6.5	6.24	5.99	0.89	0.50
34	6.75	6.49	6.24	1.13	0.75
35	7	6.74	6.49	1.38	1.00
36					
37		Impervious boundary			
38		Prescribed pressure head			

(b)

Fig. 9. (a) Rectangular dam with an impermeable wall sheet: definition of problems and comparison of free surface obtained by present method; Oden and Kikuchi [9]; Lacy and Prevost [15]; and Borja and Kishnani [16]; (b) spreadsheet representation and prescribed and converged values of pressure head.

the location of free surface computed by the proposed method is in excellent agreement with those reported by other investigators.

3.2.4. Dam with a slanted face

Fig. 10a shows the problem geometry of a dam with a slanted downstream surface, and Fig. 10b displays its spreadsheet representation and the prescribed and converged values of pressure heads. As shown in Table 3, the total number of equations is 366, and the number of iterations was 325, starting from initial values equal to 0.0 and 0.15 for interior cells and bottom boundary cells, respectively. As shown in Fig. 10a, the location of free surface computed by the proposed method follows is very similar to that reported by other investigators.

3.2.5. Nonhomogeneous rectangular dam

Fig. 11a shows the problem geometry of a dam made of two rectangular blocks of different permeability, and Fig. 11b displays its spreadsheet representation and the prescribed and converged values of pressure heads. The downstream block is ten times more pervious than the upstream one (i.e. $\alpha = k_2/k_1 = 10$). Table 1 shows all the finite difference equations and spreadsheet formulae used in solving the problem, including those at the vertical interface between the upstream and downstream blocks. As listed in Table 3, the number of equation is 882, and the number of required iteration was 414, starting from initial values equal to 0.0 and 0.15 for interior cells and bottom boundary cells, respectively. As shown in Fig. 11a, the location of free surface computed by the proposed method agrees well with those reported by other investigators.

4. Discussion

The main advantage of the proposed method is its ease of implementation and application to a wide variety of practical free surface seepage problems. From an educational point of view, all the assumptions, equations, and calculation steps are clearly stated, formulated, and executed, which is rather uncommon for other nonlinear numerical techniques for free-surface seepage problems. The proposed method is not claimed to compete with more versatile commercial seepage programs, which are either based on finite differences or finite elements. As shown in Tables 3 and 4, the convergence rate of the proposed method depends on initial values and deteriorates proportionally with the number of equations; its convergence necessitates far more iterations to converge than other matrix methods based on Newton-type iterations (e.g. [16]). All the calculation examples in Figs. 3–11 were however completed within a few minutes on personal computers, making it suitable for engineering practice. The present method is not adapted for solving large systems of equations, which may exceed the maximum size of spreadsheets. Another limitation of spreadsheet calculations is that finite difference grids can only be rectangular or triangular since there are mapped onto spreadsheet cells, therefore excluding curved boundaries and inclined layer geometries. In theory, these limitations

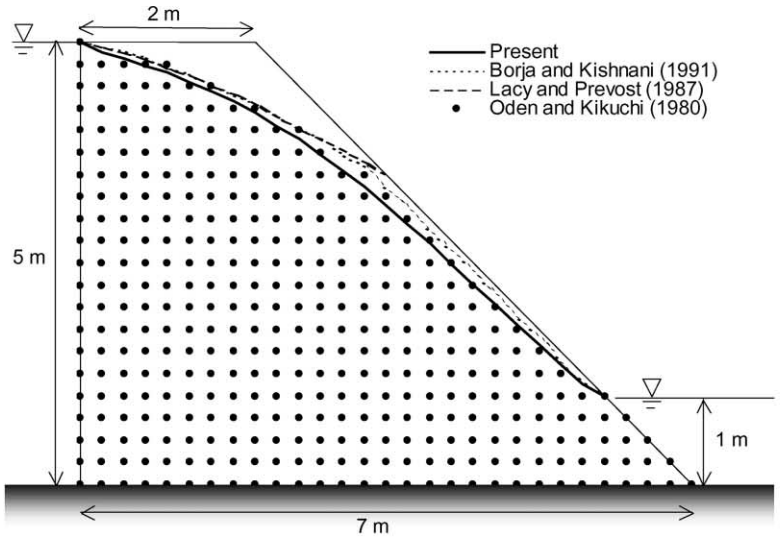

(a)

	A	B	J	K	X	Y	Z	AA	AB	AC
6	0	0	0							
7	0	0.01	0							
8	0.00	0.03	0							
9	0.25	0.16	0							
10	0.50	0.41	0.01	0						
11	0.75	0.65	0.04	0.02						
12	1.00	0.90	0.10	0.06						
13	1.25	1.14	0.26	0.15						
14	1.50	1.39	0.46	0.34						
15	1.75	1.63	0.67	0.54						
16	2.00	1.88	0.88	0.75						
17	2.25	2.13	1.10	0.96						
18	2.50	2.37	1.32	1.17						
19	2.75	2.62	1.54	1.39						
20	3.00	2.87	1.77	1.62						
21	3.25	3.11	2.00	1.85						
22	3.50	3.36	2.23	2.08						
23	3.75	3.61	2.46	2.31	0					
24	4.00	3.86	2.70	2.55	0.19	0.00				
25	4.25	4.11	2.94	2.79	0.51	0.34	0.25			
26	4.50	4.36	3.19	3.03	0.81	0.67	0.57	0.50		
27	4.75	4.61	3.43	3.28	1.10	0.97	0.87	0.79	0.75	
28	5.00	4.86	3.68	3.53	1.36	1.23	1.13	1.06	1.01	1.00
29										
30		Impervious boundary								
31		Prescribed pressure head								

(b)

Fig. 10. (a) Dam with a slanted face: definition of problems and comparison of free surface obtained by present method; Oden and Kikuchi [9]; Lacy and Prevost [15]; and Borja and Kishnani [16]; (b) spreadsheet representation and prescribed and converged values of pressure head.

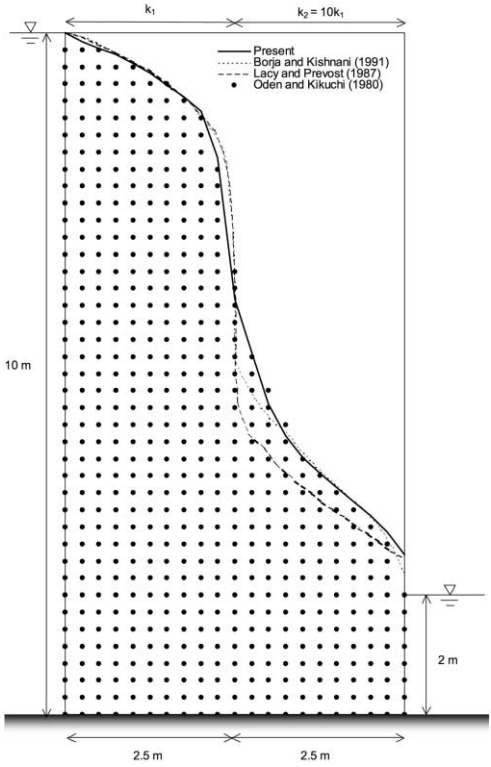

	A	B	L	V	W
6	0	0	0	0	0
7	0	0.00	0.00	0.00	0
8	0	0.03	0.00	0.00	0
9	0.25	0.15	0.00	0.00	0
10	0.5	0.39	0.00	0.00	0
11	0.75	0.62	0.00	0.00	0
12	1	0.86	0.00	0.00	0
13	1.25	1.09	0.00	0.00	0
14	1.5	1.33	0.01	0.00	0
15	1.75	1.56	0.01	0.00	0
16	2	1.80	0.02	0.00	0
17	2.25	2.03	0.02	0.00	0
18	2.5	2.26	0.03	0.00	0
19	2.75	2.49	0.04	0.00	0
20	3	2.72	0.05	0.00	0
21	3.25	2.95	0.06	0.00	0
22	3.5	3.19	0.07	0.00	0
23	3.75	3.42	0.09	0.00	0
24	4	3.65	0.10	0.00	0
25	4.25	3.88	0.11	0.00	0
26	4.5	4.11	0.12	0.00	0
27	4.75	4.34	0.13	0.00	0
28	5	4.57	0.14	0.00	0
29	5.25	4.80	0.16	0.00	0
30	5.5	5.03	0.17	0.00	0
31	5.75	5.27	0.20	0.00	0
32	6	5.50	0.25	0.00	0
33	6.25	5.74	0.34	0.01	0
34	6.5	5.97	0.45	0.01	0
35	6.75	6.21	0.58	0.01	0
36	7	6.45	0.72	0.02	0
37	7.25	6.69	0.87	0.03	0
38	7.5	6.93	1.03	0.06	0
39	7.75	7.17	1.20	0.11	0
40	8	7.42	1.38	0.22	0
41	8.25	7.66	1.57	0.43	0.25
42	8.5	7.90	1.77	0.66	0.50
43	8.75	8.15	1.98	0.90	0.75
44	9	8.40	2.19	1.14	1.00
45	9.25	8.64	2.41	1.38	1.25
46	9.5	8.89	2.64	1.63	1.50
47	9.75	9.14	2.88	1.88	1.75
48	10	9.39	3.13	2.13	2.00
49					
50		Impervious boundary			
51		Prescribed pressure head			
52		Transition zone			

(a) (b)

Fig. 11. (a) Nonhomogeneous rectangular dam with permeability varying horizontally ($\alpha = k_2/k_1 = 10$): definition of problems and comparison of free surface obtained by present method; Oden and Kikuchi [9]; Lacy and Prevost [15]; and Borja and Kishnani [16]; (b) spreadsheet representation and prescribed and converged values of pressure head.

could be overcome by breaking polygonal domains into smaller quadrilaterals and triangles mapped onto rectangular and triangular cell ranges. This type of partitioning, although it would not increase the computational time, would definitely lengthen the time required to set up equations, and might even become tedious in case of complicated geometries. The use of more advanced finite element techniques (e.g., Oden and Kikuchi [9], Lacy and Prevost [15] and Borja and Kishnani [16]) may be warranted under these circumstances.

5. Conclusion

A finite difference approach applicable to spreadsheet calculations has been proposed for calculating the solutions of unconfined seepage with an unknown free

surface. The proposed method is based on the extended pressure method for free-surface seepage problems. The finite difference equations were derived using flux conservation, which apply to a wide variety of boundary conditions and anisotropic and layered permeabilities. The main features of the proposed methods were illustrated for a one-dimensional water column, and its applicability was validated in several two-dimensional seepage problems solved in the past using more sophisticated calculation techniques. The main advantage of the proposed method is that it does not require the formation and reformation of a global matrix system to solve nonlinear systems of equations. One of its disadvantages is that the number of iterations to converge increases proportionally with the number of equations. The proposed method has not only educational values as it describes openly the equations and processes for solving free-surface seepage problems, but also practical values as it can solve many seepage problems.

References

[1] Cryer CW. On the approximate solution of free boundary problems using finite differences. Journal of the Association for Computing Machinery 1970;17(3):397–411.
[2] Taylor RL, Brown CB. Darcy flow solutions with a free surface. Journal of the Hydraulics Division, ASCE 1967;93:25–33.
[3] Finn WDL. Finite-element analysis of seepage through dams. Journal of the Soil Mechanics and Foundations Division, ASCE 1967;93(SM6):41–8.
[4] Neuman SP, Witherspoon PA. Finite element method of analyzing steady seepage with a free surface. Water Resources Research 1970;6(3):889–97.
[5] Baiocchi C. Su un problema di frontiera libera connesso a questioni di idraulica. Annali di matematica pura ed applicata 1972;91:107–27.
[6] Bathe KJ, Khoshgoftaar MR. Finite element free surface seepage analysis without mesh iteration. International Journal for Numerical and Analytical Methods in Geomechanics 1979;3:13–22.
[7] Kikuchi N. An analysis of the variational inequalities of seepage flow by finite-element methods. Quarterly of Applied Mathematics 1977;35:149–63.
[8] Alt HW. Numerical solution of steady-state porous flow free boundary problems. Numerische Mathematk 1980;31:73–98.
[9] Oden JT, Kikuchi N. Recent advances: theory of variational inequalities with applications to problems of flow through porous media. International Journal of Engineering Science 1980;18:1173–284.
[10] Friedman A. Variational principles and free-boundary problems. New York: Wiley, 1982.
[11] Desai CS, Li GC. A residual flow procedure and application for free surface flow in porous media. Advances in Water Resources 1983;6:27–35.
[12] Baiocchi C, Capelo A. Variational and quasivariational inequalities. Applications to Free Boundary Problems. New York: Wiley, 1984.
[13] Westbrook DR. Analysis of inequalities and residual flow procedures and an iterative scheme for free surface seepage. International Journal for Numerical Methods in Engineering 1985;21:1791–802.
[14] Brezis H, Kinderlehrer D, Stampacchia G. Sur une nouvelle formulation du probleme de l'ecoulement a travers une digue, Serie A. Paris: C. R. Academie des Sciences, 1978.
[15] Lacy SJ, Prevost JH. Flow through porous media: a procedure for locating the free surface. International Journal for Numerical and Analytical Methods in Geomechanics 1987;11:585–601.
[16] Borja RI, Kishnani SS. On the Solution of elliptic free-boundary problems via Newton's method. Computer Methods in Applied Mechanics and Engineering 1991;88:341–61.
[17] Bardet JP. Experimental soil mechanics. Upper Saddle River (NJ): Prentice-Hall, 1997.

[18] Darcy H. Les Fontaines publiques de la ville de Dijon. Paris: Dalmont, 1856.
[19] Varga RS. Matrix iterative analysis. Englewood Cliffs (NJ): Prentice Hall, 1963.
[20] Varga RS. Matrix iterative analysis. 2nd revised and expanded ed Springer Series in Computational Mathematics 27. New York: Springer, 1999.
[21] MS-Excel. Microsoft Corporation, 2000.